LAWRENCE
LIVERMORE
NATIONAL
LABORATORY

LLNL-JRNL-774077

Observation of a supercurrent rectifying effect intopological-insulator/normal-metal Bi1-xSbx/Pt hybrid structures

D. Qu, N. Teslich, K. Ray, G. Chapline, J. Dubois

May 13, 2019

Physical Review Letters

Disclaimer

Observation of a supercurrent rectifying effect in topological-insulator/normal-metal $Bi_{1-x}Sb_x$/Pt hybrid structures

Dong-Xia Qu, Nick E. Teslich, Keith G. Ray, George F. Chapline, and Jonathan L DuBois

Lawrence Livermore National Laboratory, Livermore, California 94550, USA

(Dated: July 25, 2019)

Abstract

We report transport evidence of nonreciprocal response in a topological-insulator/normal-metal $Bi_{0.91}Sb_{0.09}$/Pt hybrid structure. In the presence of an in-plane magnetic field, we observe a direction-dependent critical current asymmetry, which points to the occurrence of a supercurrent rectifying effect. We demonstrate that the observed magneto-transport anomaly can only arise from the topological surface states that induce a strong correlation between the spin polarization of carriers and the direction of supercurrent.

PACS numbers: 74.78.w, 73.23.-b, 74.45.+c

A two-dimensional (2D) superconductor induced at a topological insulator-normal metal interface offers a viable platform to search for interesting phenomena with Cooper pairs transported by spin-polarized surface states. It is predicted that a Zeeman field can generate a critical current asymmetry between the opposite current directions in a 2D superconductor with strong spin-orbit coupling (SOC), leading to the supercurrent rectifying effect [1–3]. The similar effect can also occur in a Josephson junction (JJ) when the normal region between two superconductors is made from materials with strong SOC [4–9]. In an external in-plane magnetic field, the Zeeman field couples to the electron momentum through SOC, which modifies the current-phase relationship by introducing a φ_0 phase-shift proportional to the Zeeman energy. If there is more than one pair of transmitting channels, the external field can induce a critical current asymmetry between the opposite current directions [4, 6, 7]. A superconducting rectifier may have applications ranging from SQUID magnetometers to quantum computing devices [10].

To generate a supercurrent nonreciprocal response, a variety of quantum materials have been investigated [11], such as non-centrosymmetric superconductors [12], topological insulators (TIs) [13–19], quantum dots [20, 21], nanowires [22–24], magnetic-impurity doped superconductors [25], and a two-dimensional electron gas with strong SOC in combination with a quantum point contact [6, 7, 26, 27]. Recent experiments on electric field-induced 2D superconductor MoS_2 have demonstrated nonreciprocal charge transport in the superconducting state, due to the absence of the in-plane inversion symmetry [12, 28]. For topological materials, the supercurrent rectifying effect has been identified in a 2D TI HgTe quantum-well when the Josephson current is carried only by the edge states in the quantum spin Hall regime [19]. However, observation of a nonreciprocal supercurrent in a 3D TI with Rashba-type spin-orbit interactions has not been reported, even after an extensive study [29–32].

In this Letter we report the observation of the supercurrent rectifying effect in a 3D-TI $Bi_{1-x}Sb_x$/Pt hybrid structure. We induce 2D superconductivity only on the top surface of a $Bi_{1-x}Sb_x$ single crystal using the focused ion beam (FIB) technique [36]. Pronounced critical current asymmetries are observed in the differential resistance $\mathrm{d}V/\mathrm{d}I$ in the presence of a weak in-plane magnetic field, implying that a net supercurrent is induced by the Zeeman field. The magnitude of the asymmetric critical current is significantly enhanced compared to the theoretical prediction for a 2D superconductor with strong SOC. We interpret this

large supercurrent nonreciprocal response as a result of the Josephon coupling between neighboring superconducting islands.

We fabricated the heterostructure by depositing a narrow 200-nm-thick Pt thin film on the surface of a $Bi_{0.91}Sb_{0.09}$ flake using FIB. The inset of Fig. 1 shows the scanning electron microscopy image of a typical device (Sample 1). Previous work shows that 2D superconductivity can be induced at the interface of Pt and $Bi_{1-x}Sb_x$ via FIB deposition [36]. The width of the Pt layer $W' = 2\ \mu m$ is much smaller than the width $W = 100\ \mu m$ of the $Bi_{0.91}Sb_{0.09}$ substrate. In this configuration, sharp multiple peaks are often observed in the differential resistance curve $\mathrm{d}V/\mathrm{d}I$. These sharp $\mathrm{d}V/\mathrm{d}I$ peaks are believed to originate from the multiple $Pt/Bi_{0.91}Sb_{0.09}$ superconducting islands generated from the spreading of Pt layer deposited beyond the intended position [36].

Compared to previous hybrid systems, our device has several important features. First, the effective mass and Fermi velocity of $Pt/Bi_{1-x}Sb_x$ superconducting regime could be close to those of normal $Bi_{1-x}Sb_x$, leading to a minimized scattering at the superconductor-normal (S-N) interface; Second, the typical thickness for our devices is $\sim 5\ \mu$m that is much larger than the superconducting coherence length of the $Bi_{1-x}Sb_x$ bulk state ξ_N^{Bulk} (~ 190 nm [36]). As a result, only the top surface and a portion of bulk should experience the proximity effect. In such a device configuration, an unpolarized bias current can produce a net spin polarization in the $Bi_{1-x}Sb_x$ surface states due to strong SOC [Fig. 1(a), top inset]. By contrast, proximity-induced superconductivity occurs on both top and bottom surfaces of a TI in most previously reported hybrid devices. The total current is not spin-polarized because top and bottom surfaces carry opposite spin.

The differential resistance $\mathrm{d}V/\mathrm{d}I$ together with the current-voltage characteristic of sample 1 measured across the electrodes L and J are shown in Fig. 1, where ΔV is obtained after subtracting a linear V-I background from V [Fig. S1, Supplementary Information (SI)]. We observe a pair of sharp peaks in the $\mathrm{d}V/\mathrm{d}I$, accompanied with an abrupt jump in the V-I trace. In Fig. 2(a), we plot $\mathrm{d}V/\mathrm{d}I$ versus T in sample 1 measured between 0.35 and 3.00 K, where the critical current I_c is defined as the current above which a sharp peak appears. We find that I_c decreases with a convex-shaped T dependence that follows the T-dependent

critical current for a short ballistic junction [37–42]:

$$I_c(T,\phi) = \frac{eN\Delta(T)}{\hbar}\frac{\tau\sin\phi}{\sqrt{1-\tau\sin^2\frac{\phi}{2}}}\tanh\left[\frac{\Delta(T)}{2k_BT}\sqrt{1-\tau\sin^2\frac{\phi}{2}}\right] \quad (1)$$

where $\Delta(T)$ is the T-dependent superconducting energy gap, N the number of propagation modes, $\hbar$ the Planck's constant, e the electron charge, ϕ the phase difference between the two superconductors, τ the angle-averaged transmission probability across the interface, and k_B the Boltzmann's constant. $I_c(T)$ is obtained by maximizing $I_c(T,\phi)$ over ϕ. With superconductor transition temperature $T_c = 2.65$ K, the Josephson coupling character (red line) is in a good agreement with the experimental data (black squares), implying that the sharp peaks arise from the Josephson coupling [Fig. 2(b)]. In addition, multiple peaks sustaining above $T = 2.65$ K gradually decrease and eventually disappear around 5 K (Fig. S2, SI), which can come from superconducting islands or the complex structure of islands with a higher transition temperature $T_c \sim 5$ K (Section 2, SI).

Next we focus on the magnetic response of the device in an in-plane magnetic field $B^{||}$ applied along the y direction. Figure 3(a) shows the differential resistance $\mathrm{d}V/\mathrm{d}I$ for sample 1 as a function of the bias current I and $B^{||}$ at 0.35 K. The critical current I_c is highlighted as the yellow/green colour, displaying pronounced asymmetries between the two current flow directions [Fig. 3(c)]. As shown in Fig. 3(b), $\mathrm{d}V/\mathrm{d}I$ (I) exhibits a particular relation $\frac{\mathrm{d}V}{\mathrm{d}I}^{+}(+B) = \frac{\mathrm{d}V}{\mathrm{d}I}^{-}(-B)$, where $+$ and $-$ represent the current direction and $+B$ and $-B$ indicate parallel magnetic field directions. Because $\frac{\mathrm{d}V}{\mathrm{d}I}$ probes the local density of states [43], our observation suggests that the field effect on the superconducting condensate should be linked to the direction of current. The nonreciprocal response has been observed in various samples fabricated and measured under the similar conditions (Section 3, SI).

In addition to the asymmetric critical current pattern, field-induced I_c enhancement is also observed. Figures 3(d) and (e) show the magnetic response of sample 2, with a thickness of 23 μm. Besides the particular symmetry relation $I_c^+(+B) = I_c^-(-B)$, the magnitude of I_c in sample 2 first decreases with increasing $B^{||}$, reaching a minimum, and then increases gradually when $B^{||}$ is larger than ~ 50 mT. It is worth noting that the enhancement of I_c with B have been reported in several topological material systems, including Al-InAs-Al JJs [44], Al-Bi_2Te_3-Al JJs [17], and Al-Cd_3As_2-Al JJs [45]. Such an enhancement is either associated with a field-induced topological phase transition or is attributed to the general

strong SOC. For our case, a more controllable sample geometry is required to further explore and clarify the underlying mechanism.

We further show that besides the sharp $\mathrm{d}V/\mathrm{d}I$ peaks, the broad $\mathrm{d}V/\mathrm{d}I$ peaks also exhibit a weak nonreciprocal response. The broad $\mathrm{d}V/\mathrm{d}I$ peaks are expected to originate from the entire superconducting layer with a width of W', e.g., $W' = 2$ μm for sample 1, because the $I_c(T)$ dependence corresponding to the broad $\mathrm{d}V/\mathrm{d}I$ peaks follows the BCS-like fit [36]. As shown in Fig. 4(a) and Fig. S9, a small but discernable asymmetric feature displays at the $\mathrm{d}V/\mathrm{d}I$ ($B^{||}$) curve measured across the electrodes J and H in sample 1. We take the current at the maxima of the broad $\mathrm{d}V/\mathrm{d}I$ peaks to be the critical current I_c. Figure 4(b) plots the asymmetric supercurrent magnitude $(I_c^+ + I_c^-)/2$ for the sharp and broad $\mathrm{d}V/\mathrm{d}I$ peaks as a function of $B^{||}$ in sample 1 at $T = 0.35$ K. $(I_c^+ + I_c^-)/2$ for samples 2 and 3 is shown in Fig. S10 of SI. We find that the magnitude of $(I_c^+ + I_c^-)/2$ for the sharp $\mathrm{d}V/\mathrm{d}I$ peaks (blue dots) is more than four times higher than that of the broad $\mathrm{d}V/\mathrm{d}I$ peak (red dots). Moreover, $(I_c^+ + I_c^-)/2$ for the broad $\mathrm{d}V/\mathrm{d}I$ peaks in sample 1 grows linearly with $B^{||}$, whereas $(I_c^+ + I_c^-)/2$ for the sharp $\mathrm{d}V/\mathrm{d}I$ peaks in samples 2 and 3 displays a dispersive shape as a function of $B^{||}$ (Fig. S10).

We may estimate the upper bound of the asymmetric supercurrent $(I_c^+ + I_c^-)/2$ induced in a 2D superconductor with strong SOC by the relation [3]:

$$I = 10^{-6}\frac{\alpha p_F \sqrt{n} B^{||} W'}{\hbar \bar{\mu}} \tag{2}$$

where α is the Rashba coefficient, $\bar{\mu}$ the chemical potential, p_F the Fermi momentum, v_F the Fermi velocity, and n the electron density. Importantly, a nonreciprocal supercurrent can only arise from surface states not bulk, because bulk states are spin-degenerate in $Bi_{0.91}Sb_{0.09}$. As shown in the inset of Fig. 4(a), the Zeeman field shifts the Fermi surfaces of the Dirac band enclosing the $\bar{\Gamma}$ point and the hole pockets in between $\bar{\Gamma}$ and $\bar{M}$ (inset of Fig. 1) along k_x in opposite directions. This induces a nonzero center-of-mass momentum in Cooper pairs, which then generates a supercurrent flow along x via the inverse Edelstein effect [1, 3, 4].

Using Eq. (2), we can fit $(I_c^+ + I_c^-)/2$ of the broad $\mathrm{d}V/\mathrm{d}I$ peaks with $\alpha p_F/\hbar\bar{\mu} = 0.2$ [black line, Fig. 4(b)]. From angle resolved photoemission spectroscopy (ARPES) measurements [46], we estimate $\alpha = 0.56$ eV Å for the surface states and $v_F = 4.3 \times 10^5$ m/s for the Dirac surface band [47–49]. If we attribute the asymmetric supercurrent at the sharp $\mathrm{d}V/\mathrm{d}I$ peaks to the same origin, the large value of $(I_c^+ + I_c^-)/2$, however, implies an enhanced α assuming

that $\bar{\mu}$ does not vary significantly across the sample. This would lead to $\alpha = 2.54$ eV Å, four times larger than the estimated value. Even though α could be enhanced at the local structure of the Pt/$Bi_{0.91}Sb_{0.09}$ interface (Section 1, SI), the large value for α could not lead to the $I_c(T)$ dependence specific to the sharp $\mathrm{d}V/\mathrm{d}I$ peaks. Hence, there should exist an additional mechanism responsible for the enhanced supercurrent asymmetry occurring at the sharp $\mathrm{d}V/\mathrm{d}I$ peaks.

Due to the complexity of the system, we briefly discuss one possible scenario based on Josephson coupling to explain the observed large supercurrent asymmetry, although alternative explanations are also possible. As illustrated in the $I_c(T)$ dependence (Fig. 2), the sharp $\mathrm{d}V/\mathrm{d}I$ features can be associated with the inter-island Josephson coupling. When the proximity effect-enlarged superconducting islands approach each other closely enough to permit Josephson currents to flow between them, a sharp peak appears in the differential resistance as a result of the transition from isolated superconducting islands to phase-coherent islands [33–36] (Section 1, SI). Moreover, the field-induced I_c asymmetries have been predicted to occur in a Josephson junction with strong SOC that transmits multiple spin-filtered channels [6, 7]. Theoretical calculation reveals that the largest asymmetries in the current-phase relation are obtained when a single resonant Andreev state coexists with a few off-resonance Andreev states [7]. That is exactly the case occurring in $Bi_{1-x}Sb_x$, in which the Dirac surface band can host a zero-energy Andreev bound state and the surface hole bands can give rise to off-resonance Andreev states (Section 6, SI). It might be the reason why pronounced I_c asymmetries have shown up in the sharp $\mathrm{d}V/\mathrm{d}I$ peaks, whereas weak I_c asymmetries display in the broad $\mathrm{d}V/\mathrm{d}I$ peaks.

In summary, we studied transport properties of a $Bi_{0.91}Sb_{0.09}$/Pt heterostructure generated from the FIB Pt deposition. Our sample configuration allows supercurrent to flow on the top surface rather than on both top and bottom surfaces, different from previously investigated 3D TI superconductor hybrid structures. We observe that the Zeeman field can induce a notable critical current asymmetry. We believe this supercurrent rectifying effect originates from the topological surface states, which behave as an effective spin polarizer to generate a supercurrent flow. Moreover, we find the magnetic field can produce a supercurrent enhancement, consistent with recent measurements of other strong SOC systems [17, 44, 45]. Our work in turn provides compelling evidence of unconventional superconducting pairing in topological surface states, establishing Pt/$Bi_{1-x}Sb_x$ as a promising platform

for exploring topological superconductivity and Majorana physics [50–52].

We would like to thank Eric R. Schwegler and Eric T. Holland for helpful discussions, and Kevin Huang and Alexander A. Baker for assistance in performing the experiments. This work was performed under the auspices of the US Department of Energy by Lawrence Livermore National Laboratory under Contract No. DE-AC52-07NA27344. The project was supported by the Laboratory Directed Research and Development (LDRD) programs of LLNL (19-LW-040 and 16-SI-004).

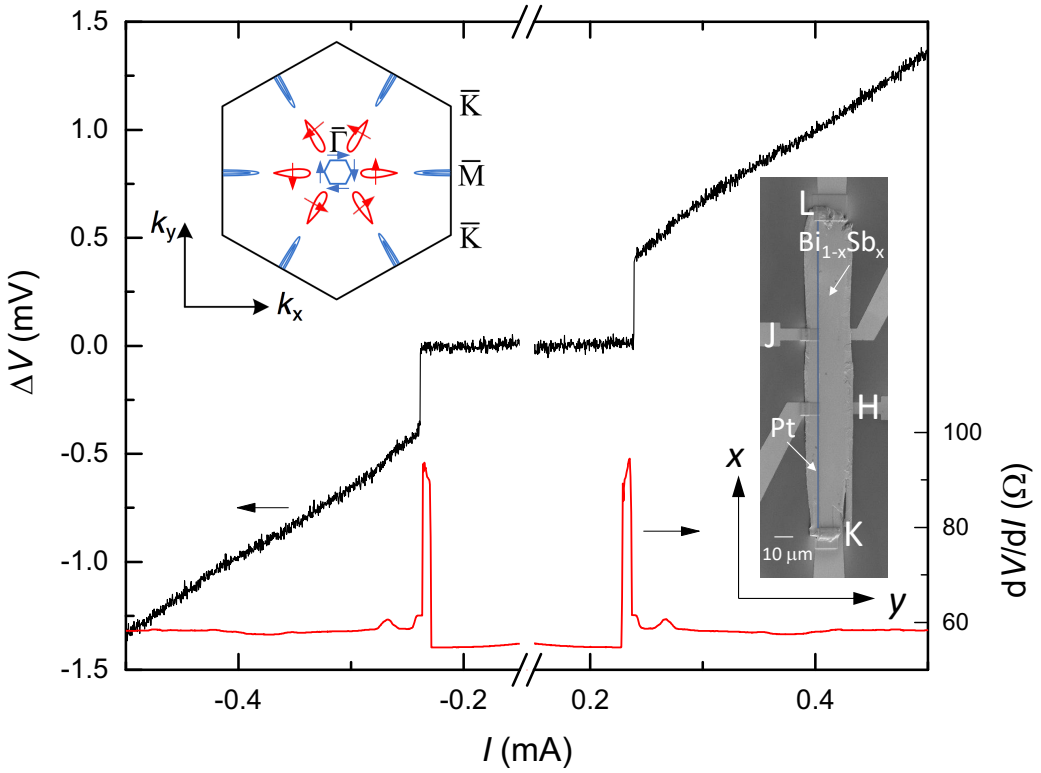

FIG. 1: Voltage and differential resistance as a function of the applied current I for sample 1 at 0.35 K, where current is injected through electrodes L and H and voltage is measured across electrodes L and J (inset). ΔV is obtained by subtracting a linear background from V. A nonhysteretic I-V characteristic is observed when sweeping the bias current up and down. Top inset: Sketch of the (111) surface Brillouin zone in $Bi_{0.91}Sb_{0.09}$ with the spin texture shown as arrows pointing to the spin direction. Right inset: Scanning electron micrograph of sample 1 with a thickness of 4.7 μm. The Pt thin film is highlighted in dark blue.

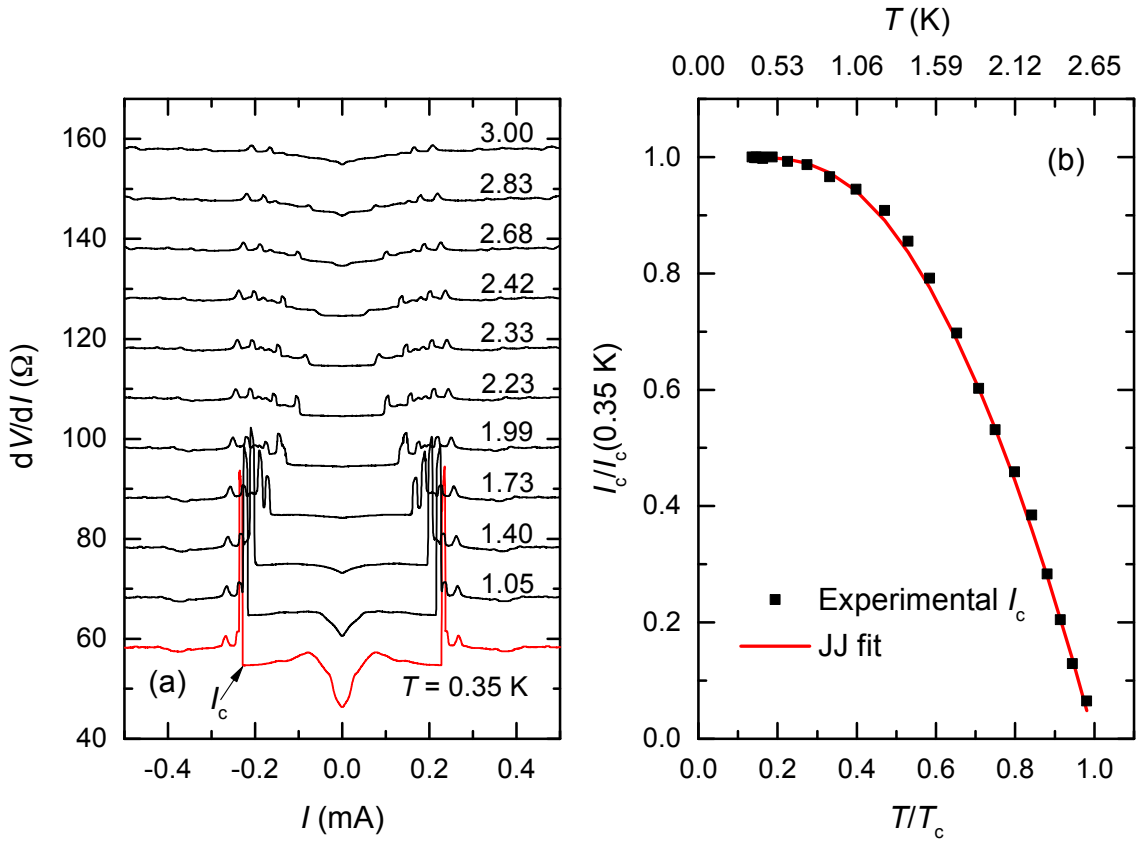

FIG. 2: (a) Temperature dependence of $\mathrm{d}V/\mathrm{d}I$ for sample 1. The arrow indicates the critical current I_c, above which the $\mathrm{d}V/\mathrm{d}I$ curve exhibits a sharp peak. (b) The normalized critical current $I_c/I_c(0.35\mathrm{K})$ as a function of the temperature with $T_c = 2.65$ K. The solid red line is a fit to the theoretical T dependence of the critical current in a short ballistic Josephson junction with the angle-averaged transmission probability $\tau = 0.15$.

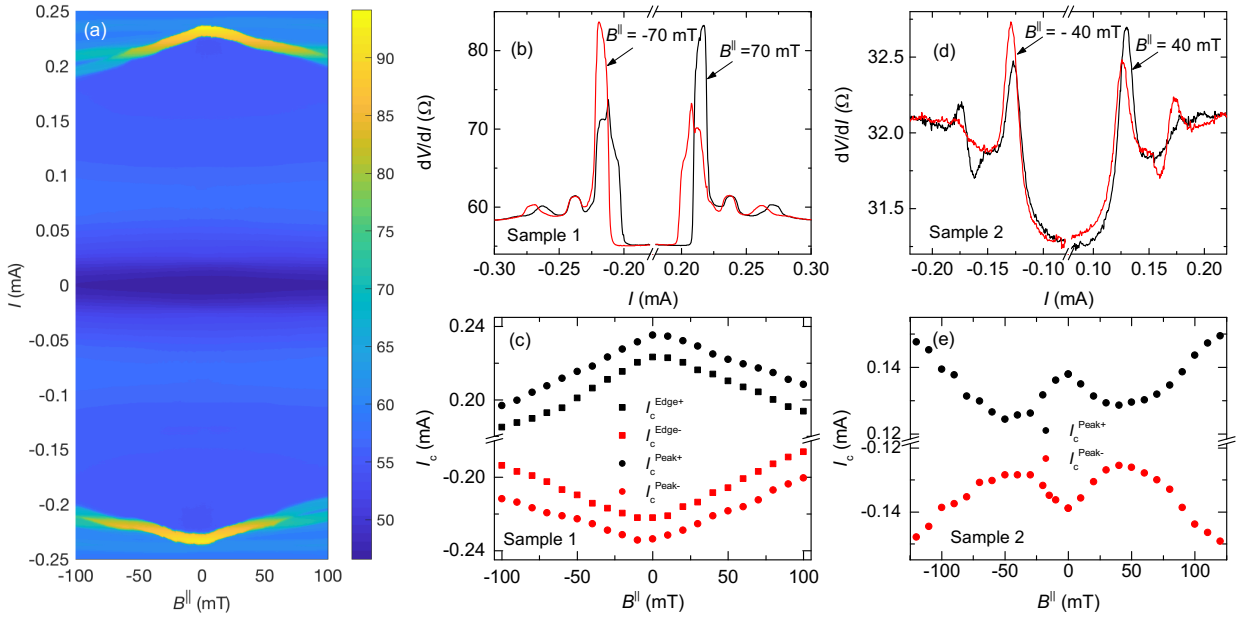

FIG. 3: (a) Differential resistance $\mathrm{d}V/\mathrm{d}I$ versus in-plane magnetic field $B^{||}$ along y direction in sample 1 (inset of Fig. 1). (b) $\mathrm{d}V/\mathrm{d}I$ as a function of current I in sample 1 at two different magnetic fields 70 and -70 mT. The critical current shows an asymmetric pattern, which we identify as a signature of the critical current rectifying effect. (c) I_c versus $B^{||}$ for sample 1 at 0.35 K. $I_c^{\mathrm{Edge}\pm}$ ($I_c^{\mathrm{Peak}\pm}$) is defined as the current above (at) which the $\mathrm{d}V/\mathrm{d}I$ displays maxima. The characteristics of the $I_c^{\mathrm{Edge}\pm}$ and $I_c^{\mathrm{Peak}\pm}$ are consistent with each other. (d) $\mathrm{d}V/\mathrm{d}I$ versus I in sample 2 at $B^{||} =$ 40 and -40 mT. (e) I_c versus $B^{||}$ for sample 2 at 0.35 K. I_c enhancement is observed for $B^{||} > 50$ mT.

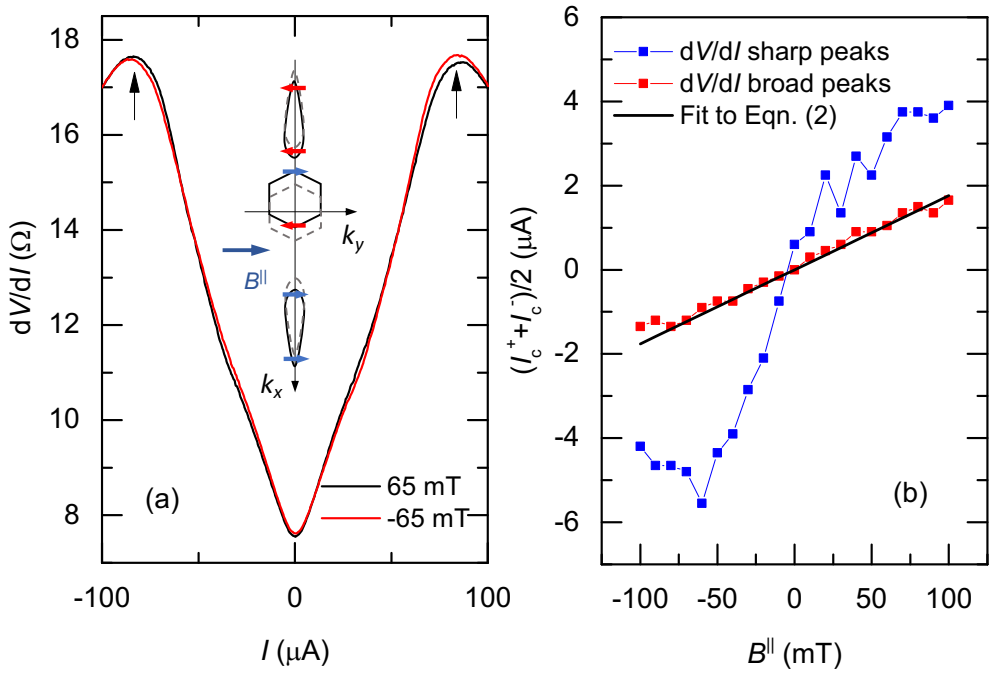

FIG. 4: (a) $\mathrm{d}V/\mathrm{d}I$ versus I measured across the center region of sample 1 for $B^{||} = 65$ and -65 mT at $T = 0.35$ K. The measurement is carried out by injecting current through the electrodes K and L and measuring the voltage through the electrodes H and J (inset of Fig. 1). The arrows indicate the slightly asymmetric $\mathrm{d}V/\mathrm{d}I$ profiles with the applied field. Inset: A Zeeman field along y shifts the Fermi surfaces of the 2D surface states in opposite directions along x. The arrows represent the spin orientation. (b) $(I_c^+ + I_c^-)/2$ as a function of $B^{||}$ identified for the sharp $\mathrm{d}V/\mathrm{d}I$ peaks (blue dots) and the broad $\mathrm{d}V/\mathrm{d}I$ peaks (red dots) in sample 1. The black line is the fit of the experimental data using Eq. (2) with $\alpha p_F/\hbar\bar{\mu} = 0.2$.

[1] V. M. Edelstein, Magnetoelectric effect in polar superconductors, Phys. Rev. Lett. **75**, 2004 (1995).

[2] L. P. Gor'kov and E. I. Rashba, Superconducting 2D System with Lifted Spin Degeneracy: Mixed Singlet-Triplet State, Phys. Rev. Lett. **87**, 037004 (2001).

[3] S. K. Yip, Two-dimensional superconductivity with strong spin-orbit interaction, Phys. Rev. B **65**, 144508 (2002).

[4] F. Konschelle, I. V. Tokatly, and F. S. Bergeret, Theory of the spin-galvanic effect and the anomalous phase shift ϕ_0 in superconductors and Josephson junctions with intrinsic spin-orbit coupling, Phys. Rev. B **92**, 125443 (2015).

[5] F. S. Bergeret, I. V. Tokatly, Theory of diffusive ϕ_0 josephson junctions in the presence of spin-orbit coupling, EPL **110**, 57005 (2015).

[6] A. A. Reynoso, G. Usaj, C. A. Balseiro, D. Feinberg, and M. Avignon, Anomalous Josephson Current in Junctions with Spin Polarizing Quantum Point Contacts, Phys. Rev. Lett. **101**, 107001 (2008).

[7] A. A. Reynoso, G. Usaj, C.A. Balseiro, D. Feinberg, and M. Avignon, Spin-orbit-induced chirality of Andreev states in Josephson junctions, Phys. Rev. B **86**, 214519 (2012).

[8] F. Konschelle and A. Buzdin, Magnetic moment manipulation by a Josephson current, Phys. Rev. Lett. **102** 017001 (2009).

[9] M. Eschrig, Spin-polarized supercurrents for spintronics: a review of current progress, Rep. Prog. Phys. **78** 104501 (2015).

[10] D. G. McDonald, Superconducting electronics, Phys. Today **34**, 36 (1981).

[11] Y. Tokura and N. Nagaosa1, Nonreciprocal responses from non-centrosymmetric quantum materials, Nat. Commun. **9**, 3740 (2018).

[12] R. Wakatsuki, Y. Saito, S. Hoshino, Y. M. Itahashi, T. Ideue, M, Ezawa, Y, Iwasa, N. Nagaosa, Nonreciprocal charge transport in noncentrosymmetric superconductors, Sci. Adv. **3**, (2017).

[13] Y. Tanaka, T. Yokoyama, N. Nagaosa, Manipulation of the Majorana fermion, Andreev reflection, and Josephson current on topological insulators, Phys. Rev. Lett. **103**, 107002 (2009).

[14] J. Nussbaum, T. L. Schmidt, C. Bruder, and R. P. Tiwari, Josephson effect in normal and ferromagnetic topological-insulator junctions: Planar, step, and edge geometries, Phys. Rev.

B **90**, 045413 (2014).

[15] F. Dolcini, M. Houzet, J. S. Meyer, Topological Josephson φ_0 junctions, Phys. Rev. B **92**, 035428 (2015).

[16] A. Rasmussen, J. Danon, H. Suominen, F. Nichele, M. Kjaergaard, and K. Flensberg, Effects of spin-orbit coupling and spatial symmetries on the Fraunhofer interference pattern in SNS junctions. Phys. Rev. B **93**, 155406 (2016).

[17] S. Charpentier, L. Galletti, G. Kunakova, R. Arpaia, Y. Song, R. Baghdadi, S. M. Wang, A. Kalaboukhov, E. Olsson, F. Tafuri, D. Golubev, J. Linder, T. Bauch, and F. Lombardi, Induced unconventional superconductivity on the surface states of Bi_2Te_3 topological insulator, Nat. Commun. **8**, 2019 (2017).

[18] C.-Z. Chen, J. J. He, M. N. Ali, G.-H. Lee, K. C. Fong, and K. T. Law, Asymmetric Josephson effect in inversion symmetry breaking topological materials, Phys. Rev. B **98**, 075430 (2018).

[19] E. Bocquillon, R. S. Deacon, J. Wiedenmann, P. Leubner, T. M. Klapwijk, C. Brüne, K. Ishibashi, H. Buhmann, and L. W. Molenkamp, Gapless Andreev bound states in the quantum spin Hall insulator HgTe, Nat. Nanotechnol. **12**, 137 (2017).

[20] A. Zazunov, R. Egger, T. Jonckheere, and T. Martin, Anomalous Josephson current through a spin-orbit coupled quantum dot, Phys. Rev. Lett. **103**, 147004 (2009).

[21] D. B. Szombati, S. Nadj-Perge, D. Car, S. R. Plissard, E. P. A. M. Bakkers, and L. P. Kouwenhoven, Josephson φ_0-junction in nanowire quantum dots, Nat. Phys. **12**, 568 (2016).

[22] T. Yokoyama, M. Eto, Y. V. Nazarov, Anomalous josephson effect induced by spin-orbit interaction and Zeeman effect, Phys. Rev. B **89**, 195407 (2014).

[23] G. Campagnano, P. Lucignano, D. Giuliano, A. Tagliacozzo, Spin-orbit coupling and anomalous josephson effect in nanowires. J. Phys. Condens. Matter **27**, 205301 (2015).

[24] A. Murani, *et al*, Ballistic edge states in Bismuth nanowires revealed by SQUID interferometry, Nat. Commu. **8**, 15941 (2017).

[25] S. S. Pershoguba, K. Björnson, A. M. Black-Schaffer, A. V. Balatsky, Currents induced by magnetic impurities in superconductors with spin-orbit coupling, Phys. Rev. Lett. **115**, 116602 (2015).

[26] A. Furusaki, Josephson current carried by Andreev levels in superconducting quantum point contacts, Superlat. and Microstruct. **25**, 809 (1999).

[27] M. Eto, T. Hayashi, and Y. Kurotani, Spin polarization at semiconductor point contacts in

absence of magnetic field, J. Phys. Soc. Jpn. **74**, 1934 (2005).

[28] Y. Saito, Y. Nakamura, M. S. Bahramy, Y. Kohama, J. Ye, Y. Kasahara, Y. Nakagawa, M. Onga, M. Tokunaga, T. Nojima, Y. Yanase, Y. Iwasa, Superconductivity protected by spinvalley locking in ion-gated MoS_2. Nat. Phys. **12**, 144 (2016).

[29] M. Veldhorst, M. Snelder, M. Hoek, T. Gang, V. K. Guduru, X. L. Wang, U. Zeitler, W. G. van derWiel, A. A. Golubov, H. Hilgenkamp, and A. Brinkman, Josephson supercurrent through a topological insulator surface state, Nat. Mater. **11**, 417 (2012).

[30] J. R. Williams, A. J. Bestwick, P. Gallagher, S. S. Hong, Y. Cui, A. S. Bleich, J. G. Analytis, I. R. Fisher, and D. Goldhaber-Gordon, Unconventional Josephson effect in hybrid superconductor-topological insulator devices, Phys. Rev. Lett. **109**, 056803 (2012).

[31] L. Galletti, S. Charpentier, M. Iavarone, P. Lucignano, D. Massarotti, R. Arpaia, Y. Suzuki, K. Kadowaki, T. Bauch, A. Tagliacozzo, F. Tafuri, and F. Lombardi, Influence of topological edge states on the properties of Al/ Bi_2Se_3/Al hybrid Josephson devices. Phys. Rev. B **89**, 134512 (2014).

[32] C. Kurter, A. D. Finck, Y. S. Hor, and D. J. Van Harlingen, Evidence for an anomalous current-phase relation in topological insulator Josephson junctions. Nat. Commun. **6**, 7130 (2015).

[33] Z. Wang, W. Shi, H. Xie, T. Zhang, N. Wang, Z. Tang, X. Zhang, R. Lortz, and P. Sheng, Superconducting resistive transition in coupled arrays of 4 $\AA$ carbon nanotubes, Phys. Rev. B **81**, 174530 (2010).

[34] B. Bergk, A. P. Petrovi, Z. Wang, Y. Wang, D. Salloum, P. Gougeon, M. Potel, and R. Lortz, Superconducting transitions of intrinsic arrays of weakly coupled one-dimensional superconducting chains: the case of the extreme quasi-1D superconductor $Tl_2Mo_6Se_6$, New J. Phys. **13**, 103018 (2011).

[35] X. Shi, W. Yu, Z. Jiang, B. A.Bernevig, W. Pan, S. D. Hawkins, and J. F. Klem, Giant supercurrent states in a superconductor-InAs/GaSb-superconductor junction, J. Appl. Phys. 118, 133905 (2015).

[36] D.-X. Qu, N. E. Teslich, Z. Dai, G. F. Chapline, T. Schenkel, S. R. Durham, and J. Dubois, Onset of two-dimensional superconducting phase in a topological-insulator-normal-metal $Bi_{1-x}Sb_x$/Pt junction fabricated by ion-beam techniques, Phys. Rev. Lett., **121**, 037001 (2018).

[37] I. O. Kulik and A. N. Omel'yanchuk, Contribution to the microscopic theory of the Josephson effect in superconducting bridges, JETP Lett. **21**, 96 (1975).

[38] C. W. J. Beenakker, Universal limit of critical-current fluctuations in mesoscopic Josephson junctions, Phys. Rev. Lett. **67**, 3836 (1991).

[39] I. V. Borzenets, F. Amet, C. T. Ke, A. W. Draelos, M. T. Wei, A. Seredinski, K. Watanabe, T. Taniguchi, Y. Bomze, M. Yamamoto, S. Tarucha, and G. Finkelstein, Ballistic Graphene Josephson junctions from the short to the long junction regimes, Phys. Rev. Lett. **117**, 237002 (1991).

[40] A. A. Golubov, M. Y. Kupriyanov, and E. Il'ichev, The current-phase relation in Josephson junctions, Rev. Mod. Phys. **76**, 411 (2004).

[41] J. Park, J. H. Lee, G.-H. Lee, Y. Takane, K.-I. Imura, T. Taniguchi, K. Watanabe, and H.-J. Lee, Short ballistic Josephson coupling in planar Graphene Junctions with inhomogeneous carrier doping, Phys. Rev. Lett. **120**, 077701 (2018).

[42] M. Kayyalha, M. Kargarian, A. Kazakov, I. Miotkowski, V. M. Galitski, V. M. Yakovenko, L. P. Rokhinson, and Y. P. Chen, Anomalous low-temperature enhancement of supercurrent in topological-insulator nanoribbon Josephson junctions: evidence for low-energy Andreev bound states, Phys. Rev. Lett. **122**, 047003 (2019).

[43] F. Zhang and C. L. Kane, Time-Reversal-Invariant Z_4 fractional Josephson effect, Phys. Rev. Lett. **113**, 036401 (2014).

[44] J. Tiira, E. Strambini, M. Amado, S. Roddaro, P. San-Jose, R. Aguado, F. S. Bergeret, D. Ercolani, L. Sorba, and F. Giazotto, Magnetically-driven colossal supercurrent enhancement in InAs nanowire Josephson junctions, Nat. Commun. **8**, 14984 (2017).

[45] W. Yu, W. Pan, D. L. Medlin, M. A. Rodriguez, S. R. Lee, Z.-q. Bao, and F. Zhang, π and 4π Josephson effects mediated by a Dirac semimetal, Phys. Rev. Lett., **120**, 177704 (2018).

[46] C. R. Ast, J. Henk, A. Ernst, L. Moreschini, M. C. Falub, D. Pacile, P. Bruno, K. Kern, and M. Grioni, Giant spin splitting through surface alloying, Phys. Rev. Lett. **98**, 186807 (2007).

[47] D. Hsieh, D. Qian, L. Wray, Y. Xia, Y. S. Hor, R. J. Cava, and M. Z. Hasan, Nature **452**, 970 (2008).

[48] D. Hsieh *et al*, Observation of unconventional quantum spin textures in topological insulators, Science **323**, 919 (2009).

[49] D.-X. Qu, S. K. Roberts, and G. F. Chapline, Observation of huge surface hole mobility in

the topological insulator $Bi_{0.91}Sb_{0.09}$ (111), Phys. Rev. Lett. **111**, 176801 (2013).

[50] L. Fu and C. L. Kane, Superconducting proximity effect and Majorana fermions at the surface of a topological insulator, Phys. Rev. Lett. **100**, 096407 (2008).

[51] A. C. Potter and L. Fu, Anomalous supercurrent from Majorana states in topological insulator Josephson junctions, Phys. Rev. B **88**, 121109(R) (2013).

[52] F. Pientka, A. Keselman, E. Berg, A. Yacoby, A. Stern, and B. I. Halperin, Topological superconductivity in a planar Josephson junction, Phys. Rev. X **7**, 021032 (2017).